

**Biomimetic Honeycomb-patterned Surface as the Tunable
Cell Adhesion Scaffold**

Journal:	<i>Biomaterials Science</i>
Manuscript ID:	BM-ART-07-2014-000233.R1
Article Type:	Paper
Date Submitted by the Author:	30-Jul-2014
Complete List of Authors:	Chen, Shuangshuang; Shanghai Jiao Tong University, School of Chemistry and Chemical Engineering Lu, Xuemin; Shanghai Jiao Tong University, School of Chemistry and Chemical Engineering Hu, Ying; Shanghai Jiao Tong University, Lu, Qinghua; Shanghai Jiao Tong University, School of Chemistry and Chemical Engineering;

ARTICLE

Biomimetic Honeycomb-patterned Surface as the Tunable Cell Adhesion Scaffold

S. S. Chen,^a X. M. Lu,^{a*} Y. Hu^a and Q. H. Lu^{a*}

Cite this: DOI: 10.1039/x0xx00000x

Received 00th May 2014,
Accepted 00th May 2014

DOI: 10.1039/x0xx00000x

www.rsc.org/

Inspired by the typically adhesive behaviors of fish skin and *Parthenocissus tricuspidata*, two different decorations of polystyrene honeycomb membrane (PSHCM) prepared by the breath figure approach were carried out with poly (N-(3-Sulfopropyl)-N-(methacryloxyethyl)-N,N-dimethylammonium betaine)(polySBMA) to explore controllable bio-adhesive surfaces. Casting and dip-coating were employed to graft polySBMA onto the plasma treated PSHCM. The polySBMA casted PSHCM showed a uniform covering layer on the PSHCM just like the mucus layer of fish skin, presenting excellent anti-fouling property. On the contrary, dip-coated one showed the polySBMA aggregating on the honeycomb pore walls forming a large number of sucking disks like adhesive disks of the tendrils of *P. tricuspidata*, which remarkably boost cell adhesion on substrates. Thus, bio-adhesion could be regulated as desired by tuning the distribution of zwitterionic polymer on the honeycomb surface. The results may provide a new approach for the design of biomaterials surface.

Introduction

Natural and artificial biomaterials are characterized by micro- and nanoscale morphologies to response various physiological environments. For example, bone tissues need an appropriate surface topography to support cell adhesion, while some organs or organ transplantations, especially blood-contacted materials such as intravascular stents, need a certain degree of roughness to prevent bio-fouling.¹⁻⁵ Thus, in the context of tissue repair and regeneration, an appropriate topological surface is an essential requirement for biomaterials.^{6, 7}

To investigate the adhesive behaviours between proteins/cells and surfaces, topological surfaces that mimic the natural ones have recently attracted much interest.⁸⁻¹⁰ Different morphologies such as grooves, pits, pillars have been investigated.¹¹⁻¹⁵ The morphological parameters that affect cellular behaviours, including the density, shape and size, have been systematically studied.^{11, 13, 16} It has become increasingly apparent that a rough surface can stimulate cell adhesion and encourage cell differentiation.¹⁷ However, most above-mentioned morphologies require elaborate and complex preparation.^{18, 19} Hence, it makes sense to develop a more convenient method to fabricate surface topographies. Breath figure as a water-driven template method has been utilized to prepare ordered hexagonally arranged pores, so called honeycomb structure.²⁰⁻²⁵ Compared with traditional patterning techniques, such as microcontact printing and dip-pen lithography, breath figure avoids specialized machinery or specifically designed templates, allowing for control of the structural properties.^{26, 27} For the porous character of honeycomb structure, various cells, such as hepatocyte, fibroblast, stem cell, and so on, have been widely investigated.²⁸⁻³³ It has been demonstrated that the honeycomb structure can greatly affect the cell adhesion, spreading and

differentiation. In microscale aspect, the micropatterning protein has been successfully fabricated on the honeycomb structures.^{34, 35} However, to the best of our knowledge, the tunable bio-adhesion based on honeycomb surface has not hitherto been reported.

Apart from the topological influence, the chemical component is another vital factor that affects the bio-adhesive behaviors.³⁶ Surface modification with hydrophilic polymers, such as poly (ethylene glycol) (PEG), poly (hydroxyethyl methacrylate) (PHEMA), poly (oligo(ethylene glycol) methacrylate) (POEGMA), has proved to be an efficient approach for changing the adsorption properties of non-specific proteins.³⁷⁻³⁹ Recently, zwitterionic polymers have received much attention because of the stability of their surface properties and high efficiency as antifouling materials.⁴⁰⁻⁴² Cellular attachment, spreading, and protein adsorption were resisted on the zwitterionic polymer surface, demonstrating that super-low fouling ability had been achieved.

In nature, many of unique skills of animals and plants benefit from the coordination of the surface components and microstructures on their bodies.^{43, 44} It is well known that the smooth and soft mucus layer on fish surfaces endows its skin with prominent anti-fouling ability regardless of skin topologies.^{44, 45} Thus a promising strategy to decrease bio-contamination is to obtain a smooth hydrophilic layer. Whereas the self-clinging *P. tricuspidata* can climb on house-outside walls with tendrils to obtain vertical growth. At the end of tendrils, a great deal of adhesive disks exist with porous surface appearance, through which the suction force was provided: the adhesive disks secrete a heavy sticky fluid when stimulated, the chemical anchor of the sticky fluid and negative pressure of the adhesive disks make themselves attach quite firmly to house walls.^{46, 47}

Inspired by the nature, a tunable bio-adhesion surface based on honeycomb structure was explored in this work. A honeycomb structure prepared by the breath figure technique was decorated with zwitterionic polymer. Two different micro-distributions of the zwitterionic polymer (polySBMA) on the honeycomb surface were obtained, namely the fish surface- or tendrill-like figures. The results of bio-adhesion experiments showed that the two figures presented the different adhesion behaviors. Anti-fouling surface as fish scales and highly adhesive surface as tendrils of *P. tricuspidate* demonstrated that the bio-adhesion properties of honeycomb-patterned surfaces could be tunable by controlling the distributions of zwitterionic polymer.

Experimental

Materials.

Polystyrene (PS, Mw=250k) was purchased from Acros Reagents. N-(3-Sulfopropyl)-N-(methacryloxyethyl)-N,N-dimethylammonium betaine (SBMA, 97%) was obtained from Sigma-Aldrich. Rhodamine B (Rh-B, 95%) was purchased from J&K Chemical Ltd. Toluene and other reagents were obtained from Sinopharm Chemical Reagent Co. HeLa cells were obtained from the Cell Resource Centre of Life Sciences in Shanghai. Bovine serum albumin (BSA, 66kD, >98%), fetal bovine serum (FBS), and Dulbecco's modified Eagle medium (DMEM) were obtained from Gibco BRL. Cellular staining dyes and all other cell culture reagents were purchased from the Beyotime Institute of Biotechnology. Water used in the experiments was purified with a Hitech system to reach a resistivity of above 18.2 M Ω •cm.

Preparation of PS Honeycomb Membrane

PS honeycomb membranes were prepared through a typical breath figure approach.²² Firstly, a 10×10 mm glass slide was treated with Piranha solution at 120 °C for 30 min to remove impurities. PS was dissolved in toluene at a concentration of 1 mg/mL, and 40 μ L of this solution was coated onto the pretreated glass, with humid air (approximately 70% R.H., 4 L/min) flowing across the surface in a home-made chamber. All processes were performed at room temperature. As a comparison, a flat PS membrane was prepared by solvent self-evaporation in a dry chamber.

Surface Modification of the PS Honeycomb Membranes

The PS honeycomb membranes were exposed to O₂ plasma at room temperature and a pressure of 40 Pa for 3 min using an SY-DT01 plasma apparatus (Suzhou OPS Plasma Technology, Co.), which endowed them with surface radicals. The surface modification procedure is shown schematically in Fig. 1. Two methods were then utilized for the grafting of polySBMA, namely casting and dip-coating. The casting process was as follows: 20 μ L of a 10%wt aqueous SBMA solution was directly cast onto the surface by means of a syringe. A UV-induced grafting technique was then applied to accelerate the reaction of SBMA with the surface radicals. The UV light generator (Intelli-ray 600, China) was set at 365 nm with energy 35 Mw/cm² and the exposure time was limited to 5 min. Dip-coating treatment was performed in a dip-coater (Panasonic, Japan); the dipping time and dragging speed were optimized at 5 min and 10 cm/min, respectively. After dip-coating of SBMA, the membranes were irradiated with UV light for 1 min with energy 35 Mw/cm². For convenience, the

two modified membranes were named as casting and dip-coating membranes, respectively.

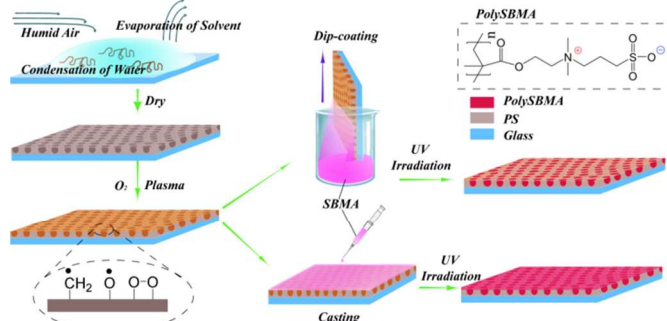


Fig. 1 Schematic illustration of the fabrication process of zwitterionic polySBMA grafted onto the honeycomb PS membrane: a highly ordered honeycomb membrane was prepared by the breath figures method; plasma treatment was then applied to generate surface radicals. The SBMA solution was introduced onto membrane by casting and dip-coating. Finally, UV irradiation was then utilized to enhance the grafting reaction of polySBMA.

Characterizations

The chemical properties of the membranes were characterized by Fourier-transform infrared spectroscopy (FTIR, Perkin-Elmer, Spectrum 100, USA), attenuated total reflectance Fourier-transform infrared spectroscopy (ATR-FTIR) and X-ray photoelectron spectroscopy (XPS, PHI-5000 Versaprobe II, Japan). In order to avoid the interference of glass slide, all the membranes were peeled off from glass slides and attached onto a KBr tablet, then submitted to FTIR measurement. The scanning area of XPS was 200×200 μ m. Scanning electron microscopy (SEM) images were acquired using an FEI Nova NanoSEM (FEI, USA). The swollen morphologies of the membranes under water were imaged using a Leica DM 4000 optical microscope (OM) equipped with a CCD camera (Leica, Germany). In addition, the Rh-B labelling was applied to track the distribution of polySBMA. The membranes were firstly immersed in 10 μ g/mL of Rh-B for 1h at room temperature, then observed with an inverted fluorescence microscope (IX 71, Olympus) equipped with a CCD camera. The wettability measurement was performed on an OCA 20 apparatus (Dataphysics, Germany).

Protein Adsorption

For the adsorption of BSA, membranes were first rinsed five times with phosphate-buffered saline (PBS, pH 7.4) and then immersed in PBS for 12 h to achieve swelling equilibrium. The membranes were then transferred to a 24-well plate and incubated with 1 mL of a 5 mg/mL solution of BSA in PBS for 2 h at 37 °C. Subsequently, the membranes were transferred to a new plate filled with 1 mL of PBS containing 1 wt.% Triton X-100. The adsorbed proteins were desorbed by sonication for 20 min. The protein concentration was quantitatively measured by a bicinchoninic acid protein assay (BCA). For this, 20 μ L of desorbed protein solution was mixed with 200 μ L of BCA reagent in a 96-well plate and incubated for 30 min at 37 °C. Finally, the light absorbance at wavelength 570 nm was determined using a microplate reader. The absorbance of each sample was measured six times. A standard curve was then plotted. Additionally, the surface morphology of the membranes after adsorption of the protein was detected by atom force microscopy (AFM, BioScope, VEECO).

Cell Culture

The membranes were sterilized with medicinal alcohol and exposed to UV light for 24 h, then placed in a 24-well plate and rinsed with PBS (2×1 mL). HeLa cells were cultured in DMEM with 10% FBS and 1% penicillin-streptomycin, seeded at a density of 4×10^4 cells per well, and incubated at 37 °C in atmosphere containing 5% CO₂ for 24 h. The membranes with adhered cells were then rinsed twice with PBS to remove unattached cells. The cell viability was assessed by dead/live (AO/EB) double staining. An inverted fluorescence microscope (IX 71, Olympus) equipped with a CCD camera was used for cell imaging. Cell counting and image overlay were carried out with Image J software. SEM was also used for cellular morphology analysis. Cells were fixed with 2.5% glutaraldehyde solution for 20 min and then dehydrated with graded ethanol solutions. Samples were sputtered with Pt and examined with an FEI Nova NanoSEM 450 (FEI, USA).

Results and discussion

Chemistry and Wettability of membranes

FTIR was applied to characterize the zwitterionic polymer decorated honeycomb membranes as shown in Fig. 2. The bands at $\nu=1180$ and 1020 cm⁻¹ can be assigned to asymmetric and symmetric vibrations of the sulfonyl group ($-\text{SO}_3$) and the peak at 1720 cm⁻¹ is the characteristic peak of carbonyl group ($\text{C}=\text{O}$) both decorated membranes (c and d) exhibited the characteristic bands of polySBMA, confirming the successful grafting of the zwitterionic polymer. Moreover, an obvious difference in intensity of the two characteristic peaks, where the stretching vibration peak of $\text{C}=\text{C}$ in the benzene ring ($\nu=1490$ cm⁻¹) is chosen as a reference, could be seen in the spectra of the two decorated membranes: the peak intensity in the spectrum of the casting membrane was stronger than that in the spectrum of the dip-coating membrane, implying a difference in SBMA grafting density. Same results were also observed in ATR-FTIR spectrum (Figure S1).

In addition, N, S, and O atoms could be observed in the XPS spectra of both the dip-coating and casting PSHCM, furthermore demonstrating the success grafting of polySBMA on the membranes (Fig. 3). The peak information was summarized in Table S1.

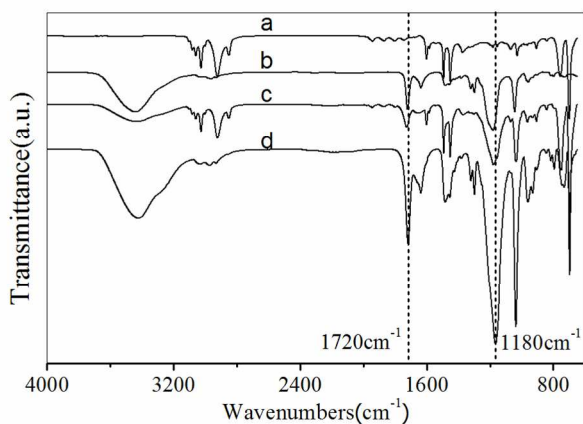


Fig. 2 FTIR spectra of the membranes: a) spectrum of the PS honeycomb membrane without modification, b) spectrum of the SBMA monomer, and zwitterionic polymer-modified membranes obtained by c) dip-coating and d) direct casting.

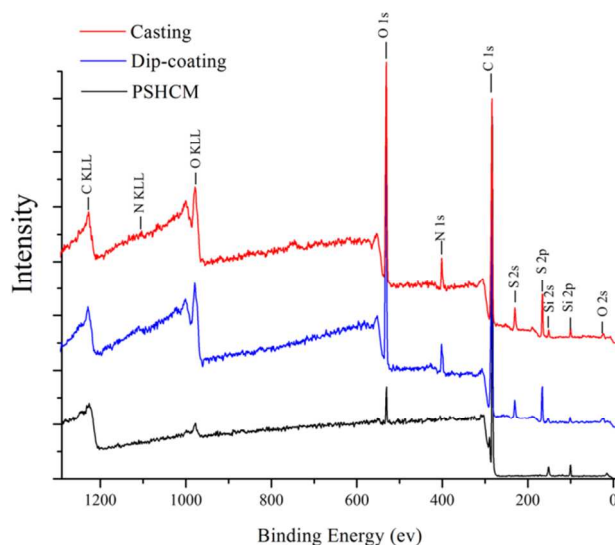


Fig. 3 XPS spectra of the membranes. red) the casting membrane; blue) the dip-coating membrane; black) PSHCM.

The wettability was evaluated by static contact-angle measurement. As shown in Fig. 3a, the water contact angles on the undecorated flat surface and honeycomb surface were 97.2° and 106.2°, respectively. According to Wenzel theory, rough surface can increase the hydrophobicity of hydrophobic surface (water contact angle greater than 90°) and the hydrophilicity of hydrophilic surface (water contact angle less than 90°), honeycomb structure endowed PS surface with a surface roughness. Thus, honeycomb holes enhanced the hydrophobicity of the membrane.⁴⁸ After decoration with polySBMA, the contact angles of casting and dip-coating membranes were 30.5° and 25°, respectively. The slight difference in wettability of the casting and the dip-coating membranes was caused by different surface structures, as shown in Fig. 5 (b, c). The surface of the dip-coating membrane still retained porous structure, whereas that of the casting membrane was fully covered with polySBMA.

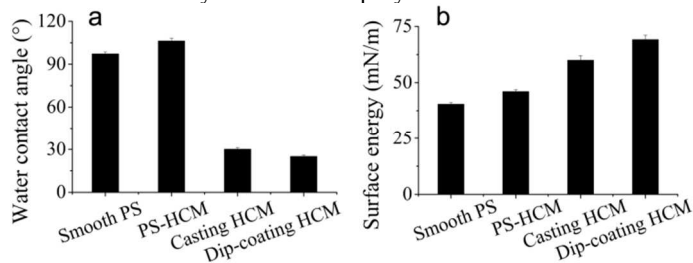


Fig. 4 Static water contact angles and surface energies of the membranes. Smooth PS and PS-HCM represent the PS flat and PS honeycomb membranes, Casting HCM denotes the polySBMA-modified honeycomb PS membrane obtained by casting, and Dip-coating HCM denotes the polySBMA-modified honeycomb PS membrane obtained by dip-coating.

The surface energy of membranes was calculated via OWRK method, based on the contact angle results of water and diiodomethane (SI). The results are shown in Fig. 4b. The undecorated PS membrane exhibited low surface energy; after the grafting of polySBMA, the surface energy increased from 40 mN/m to approximately 70 mN/m. Moreover, there was a 17% increase in surface energy of the dip-coating membrane compared with the casting membrane. The difference in surface

energy between casting and dip-coating membranes plays an important role in the process of protein adsorption and cell adhesion (vide infra).

Morphologies of the Membranes

The morphologies of the membranes were firstly characterized by SEM, as shown in Fig. 5 (a-c). Fig. 5a shows an ordered honeycomb membrane. When SBMA was casted onto the membrane (Fig. 5b), the whole pores of PSHCM were filled with polySBMA due to sufficient amount of reactive monomers and the membrane became smoother than that before casting

treatment, indicative of total coverage of the honeycomb structure with a uniform polySBMA layer. The cross-section SEM of this membrane further proved this result. By contrast, polySBMA aggregatively grafted around the wall of honeycomb hole by dip-coating (Fig. 5c) attributing to the capillary force. (Figure S2) The whole figures of cross-section SEM photographs were provided in Figure S3. The phenomena that honeycomb structure was filled with polySBMA by casting and it would exist after dip-coating can be further demonstrated by AFM (Figure. S4).

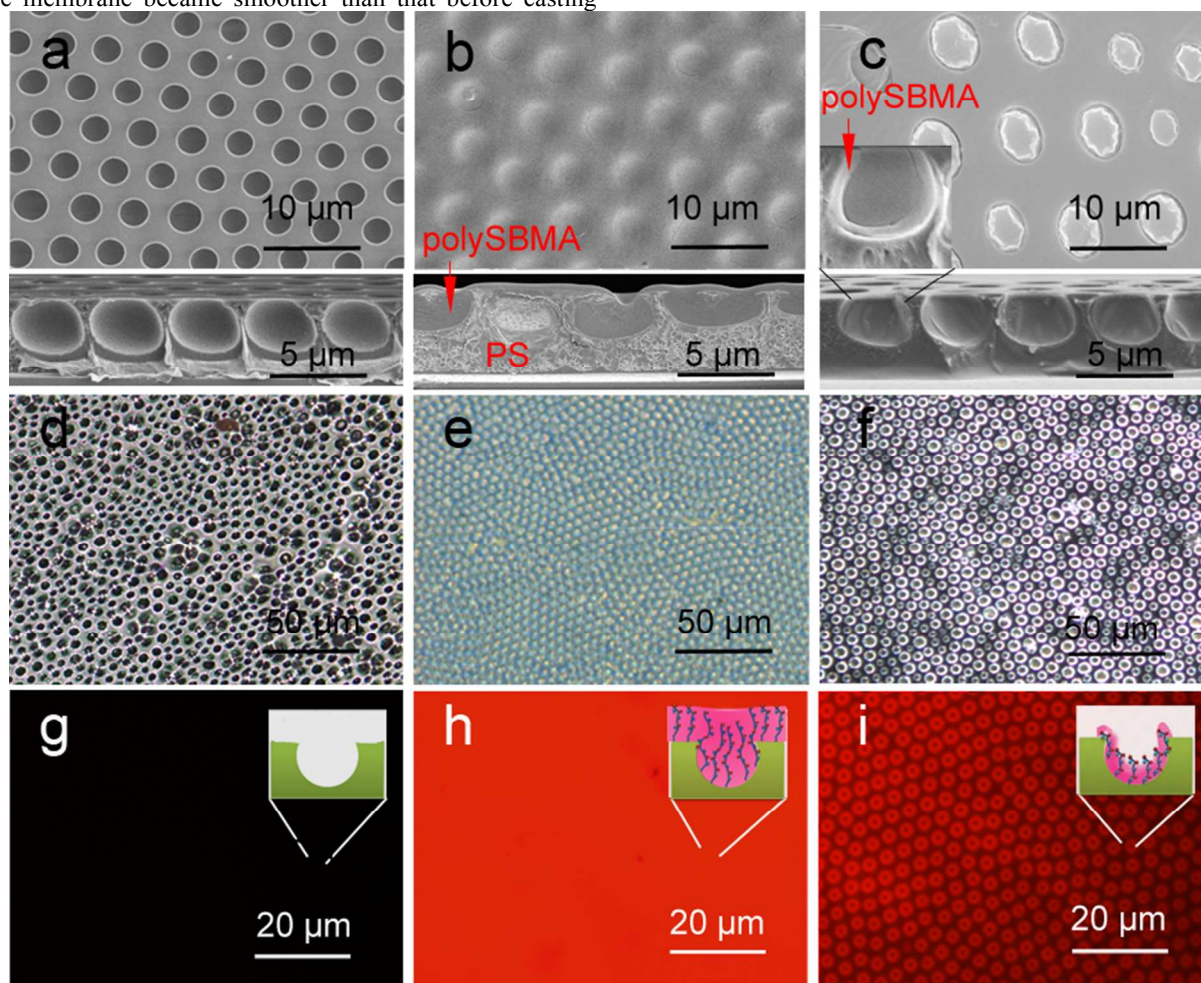


Fig. 5 SEM, OM, and fluorescence photographs of honeycomb membranes: a), b), c) SEM images; the inserted photographs are the correspondent cross-section SEM, the whole figure showed in figure s3. d), e), f) OM photographs in water; g), h), i) fluorescence images of membranes after labelling with Rhodamine ; a), d), g) honeycomb membrane without modification; b), e), h) casting membrane; c), f), i) dip-coating membrane.

Generally, the process of membranes interacting with proteins or cells is performed in aqueous media, and the swollen morphologies of the membranes directly influence cellular behavior.⁴⁹ In order to characterize the swollen morphologies of decorated membranes in water, we utilized an optical microscope (OM) to observe the morphologies of the membranes. As shown in Fig. 5d, the honeycomb PS membrane was hydrophobic and could not be significantly infiltrated. Water could not enter its pores and just formed several liquid film caps over the membrane. The casting membrane that PSHCM was fully covered with polySBMA displayed distinct swelling behaviour, namely forming a hydration layer. The dip-

coating membrane still contained the honeycomb porous structure. However, the polySBMA aggregated around the pore walls of the honeycomb and only these domains can swell in water. An ordered array of zwitterionic polymer rings was formed. Because the hydrated layer is transparent, it is difficult to distinguish the difference of the two samples just using OM. For this, fluorescent labelling method was applied to characterize the distribution of zwitterionic polymer on the surface. In this work, a water-soluble Rh-B with excitation wavelength 552 nm was selected to label the polySBMA on the surface. The zwitterionic polymer contained a large number of ammonium ($-\text{NH}_2^+$) and sulfonic ($-\text{SO}_3^-$) groups, which could

combine with the fluorescent dye. In contrary, the PS does not interact with Rh-B. Thus the Rh-B labelling can be applied to exhibit the distribution of polySBMA. The results are shown in Fig.5 (g-i). The undecorated honeycomb membrane could not interact with Rh-B and so could not emit fluorescence showing a dark image (Fig. 5g). However, the casting membrane exhibited a uniform fluorescence emission. This phenomenon suggested that the honeycomb structure had been fully covered with polySBMA (Fig. 5h). The dip-coating membrane emitted fluorescence only around the pores indicating the enrichment of polySBMA in the pore (Fig. 5i). Namely, the polySBMA aggregated around the honeycomb structure. In this case, the different decoration procedures gave rise to different distributions of the zwitterionic polymer. These composite architectures could then be utilized to investigate the interactions between cells and these surfaces.

Protein Adsorption

The adhesion of cells essentially corresponded to the adsorption of proteins, because the extracellular matrix (ECM) is made up of all kinds of proteins.⁵⁰ To study cellular behaviours on the membranes, the adsorption of BSA was utilized to investigate the interactions between proteins and surfaces.

It is well known that hydrophobic surfaces benefit protein adsorption.⁵¹ An effective method for reducing the nonspecific adsorption of proteins is to improve the wettability of surfaces. In this work, the original PSHCM surface was hydrophobic, but was rendered hydrophilic by decoration with the zwitterionic polymer. Fig. 6 (a-e) shows AFM images of membranes after the adsorption of BSA. Both the smooth and honeycomb PS membranes showed obvious protein adsorption, which can be attributed to their hydrophobicity. When the PS surfaces with or without honeycomb structures were decorated by grafting the zwitterionic polymer by casting, they exhibited repelling protein fouling. Two basic mechanisms of antifouling, namely steric repulsion and hydration theory, have been proposed.^{41, 52}

The former supposes that hydrophilic polymers bind with water through hydrogen bonds and swell, and the swollen polymer acts as a barrier that prevents proteins from attaching to the substrates; the hydration theory regards the hydration layer as an excellent antifouling barrier, because the displacement of bound water (ice-like water) molecules constitutes a major barrier in the adsorption and adhesion phenomena to highly hydrophilic surfaces.⁵³ In our works, the zwitterionic polymer layer by casting can strongly bond with water through hydrogen bonds and electrostatic interactions and form a thick hydration layer. The thick zwitterionic polymer-water layer looks like being fish scales efficiently reducing the adsorption of proteins. A significant increase in protein adsorption was observed on dip-coating membrane, as shown in Fig. 6e. To quantitatively compare the protein adsorptions on the different membranes, the BCA assay was used to detect the adsorption of BSA quantity (Fig. 6f). The protein adsorption on the hydrophobic PSHCM surface was as high as 15 g/cm², but decreased when the surface was covered with the zwitterionic polymer by casting. However, the BSA adsorption on the dip-coating membrane maintained a high level. As shown in Fig. 5c and f, we can find that polySBMA mostly aggregated around the pore walls, forming sucker disks as the adhesive disks of the tendril of self-clinging *P. tricuspidate*. The distribution of the zwitterionic polymer on the honeycomb surface prevented the formation of a uniform hydration layer. Moreover, the surface of the honeycomb structure partially retained the properties of uncovered PS, which imparted high surface energy because the

PS surface was treated with O₂ plasma before grafting polySBMA. The sucker disk structure with high surface energy caused that proteins underwent conformational changes and entropy gained upon adsorption on solid surfaces,⁵⁴ and the protein affinity on the dip-coating surface was obviously higher than that on the casting membrane. Besides, the protein adsorption on the PSHCM was different from that on the dip-coating membrane. Due to hydrophobic interaction, the protein on PSHCM was physically adsorbed as shown in Fig. 6b and e.

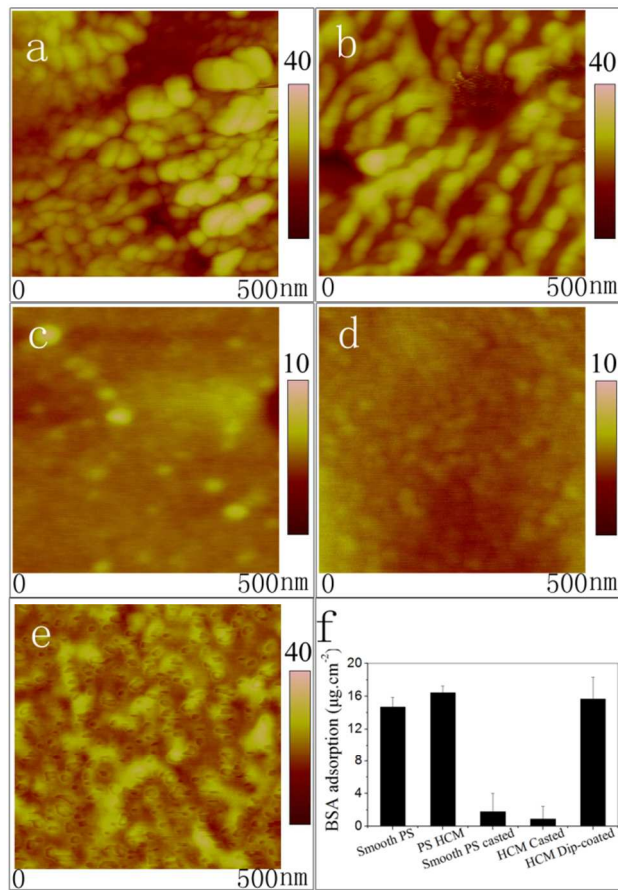


Fig. 6 AFM photographs of membranes after adsorption of BSA: a) smooth flat PS; b) the PS honeycomb membrane; c) polySBMA-modified flat PS obtained by casting; d) polySBMA-modified membrane obtained by casting, and e) polySBMA-modified membrane obtained by dip-coating. f) The results of BSA protein adsorption experiments, measured by the BCA method: smooth PS is the PS flat surface, PSHCM, smooth PS casted the polySBMA grafted PS flat, HCM casted is the casting membrane and HCM dip-coated is the dip-coating membrane.

Cell Adhesion

The HeLa cells adhered on the membranes were counted based on the fluorescence images. As shown in Fig. 7, the cell density on the PS honeycomb was 53 cells/mm². Few cells were found on the polySBMA-covered surface. Compared with the casting membrane, the dip-coating showed excellent cell adhesion (443 cells/mm²). Thus, a remarkable phenomenon was described that the PSHCM could be modulated into cell-phobic or cell-philic by regulating the surface distribution of polySBMA on the honeycomb membrane.

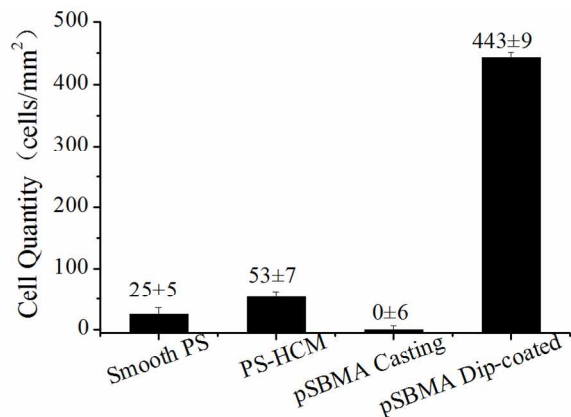


Fig. 7 Adhesion densities of HeLa cells on the surfaces after culturing for 24 h.

To acquire more detailed information of the HeLa cells on the polySBMA decorated PS honeycomb, the cells were fixed with glutaraldehyde and observed by SEM. For comparison, SEM images of the cells and the corresponding fluorescence images are shown in Fig. 8. The cells adhered on PSHCM were mostly tower-shaped and formed visible lamellipodia. Because the PSHCM was hydrophobic, a further spreading of cell is seldom to be found. Notably, there was not cell can be observed on the casting membrane due to the hydration layer.

However, on dip-coating membrane, the cells clearly spread and protrusions of different cells interconnected. The

honeycomb pores were almost covered with the cell protrusions, the cells were firmly immobilized on the dip-coated PSHCM. In contrast to the casting membrane, the polySBMA patterned surface was cell-philic due to the lack of a hydration layer.

To understand the cellular behaviour on the surfaces, we postulated that there are two possible ways of attaching cells onto the zwitterionic polymer decorated surfaces, as shown in Fig. 9. As mentioned above, polySBMA has already covered the honeycomb structure on casting membrane and uniformly form a hydration layer.⁵⁵ And the hydration layer just like the mucus layer on fish scales, which prevented proteins and cells from attaching to the surface.

While the polySBMA only aggregated around the pore walls and formed sucker disks as the adhesive desks on the tendrils of *P. tricuspidate*. The structured membranes not only hindered the formation of a uniform hydration layer but also provided favourable conditions for both protein adsorption and cell adhesion. In addition, the cavities part of honeycomb structure can provide negative pressure.⁵⁶ It is hard for cell to escape from the dip-coating membranes after the cells cover the honeycomb surface. Thus, the cells were stabilized on the dip-coating surface. In contrast, the honeycomb structure without zwitterionic polymer decoration was hydrophobic and showed a higher level of protein adsorption. Besides, the cytomembrane is hydrophilic; an appropriately hydrophilic surface is required for the permeation of culture medium and the growth of cell.⁵⁷ The hydrophobicity of the PSHCM restricted the spreading of the cells (Fig. 9).

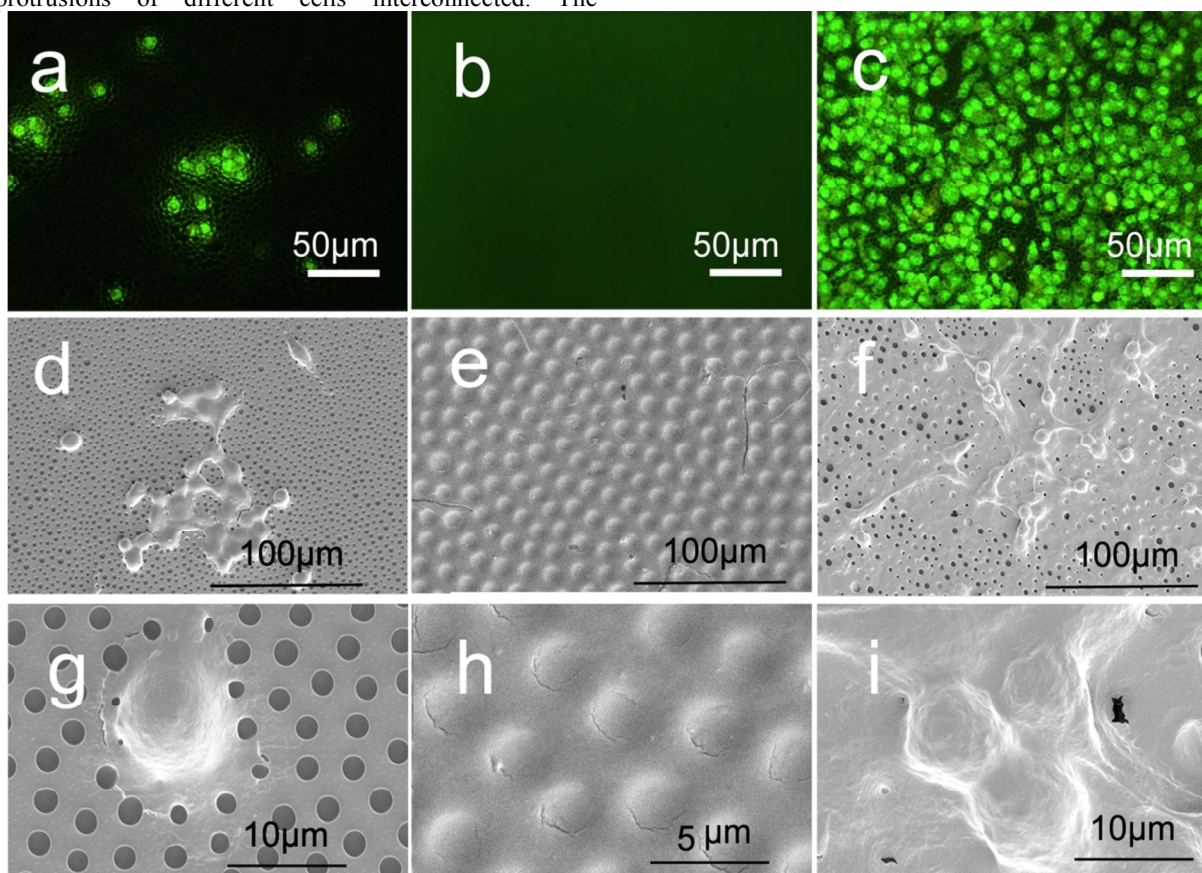


Fig. 8 AO/EB double-staining fluorescence images and SEM photographs of HeLa cells on the membranes. a)-c) Fluorescence images; d)-i) SEM photographs of HeLa cell adhesion on the membranes, where a), d), g) show the honeycomb PS membrane, b), e), h) show the polySBMA cast membranes, and c), f), i) show the polySBMA dip-coated membranes.



Fig. 9 Schematic illustration of cell behaviors on the different membranes. Cells on the undecorated HCM surface were spherical whose spreading was restricted; then two different decoration of polySBMA was process on it, namely dip-coating and casting. The dip-coating PSHCM endowed PSHCM with a Parthenocissus-like topological surface, resulting in cell-philic, while a confluent polySBMA layer formed on the casting one, which can form a hydration layer to keep cell from adhering, which was inspired by the fish surfaces.

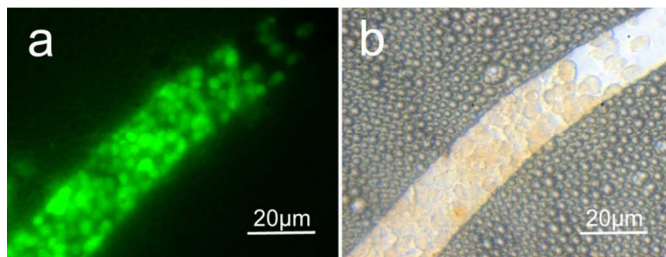


Fig. 10 AO/EB double-staining fluorescence images of cells on a designed PSHCM model. The PSHCM was coated with polySBMA by casting, and then a channel was cut with a needle.

Based on the above results, a simple pattern on the surface was created to prove the controllable cellular adhesion on the modified membrane: the honeycomb membrane with cast polySBMA was selected as the substrate, and then a channel was made with a needle. The cells were seeded onto the membrane. The results are shown in Fig. 10 and provide clear evidence that the area of the PS honeycomb membranes fully covered with polySBMA had antifouling ability. The HeLa cells adhered selectively in the channel, where substrate was not covered with polySBMA.

Conclusions

Inspired by nature, tunable bio-adhesive membranes, including highly adhesive and anti-fouling surface, were prepared based on a PS honeycomb structure, two methods have been applied to graft polySBMA onto the surface, namely directly casting and dip-coating, which gave rise to different bio-adhesive behaviors. The casting membrane showed super-low protein- and cell-binding properties. In contrast, on the dip-coating membrane, most of the polySBMA aggregated around the pore walls. In this case, the surface of the PSHCM membrane was protein- and cell-philic. Because of the array of pores, the breath figure method offers a facile route to mimic biosurfaces. Here, we have decorated the honeycomb surface to render it either cell-phobic or cell-philic by regulating the grafting of polySBMA and our results may be applicable to the design of many biomedical surfaces.

Acknowledgements

This work was supported by Major Program of Chinese National Programs for Fundamental Research and Development (973 project: 2012CB933803); National Science Fund for distinguished Young Scholars (50925310), The National Science Foundation of China (51173103, 21374060), and the Excellent Academic Leaders of Shanghai (11XD1403000).

Notes and references

^a School of Chemistry and Chemical Engineering, Shanghai Jiao Tong University, Shanghai, 200240, P.R. China.

*Tel: +86 21 54747535; Fax: +86 21 54747535

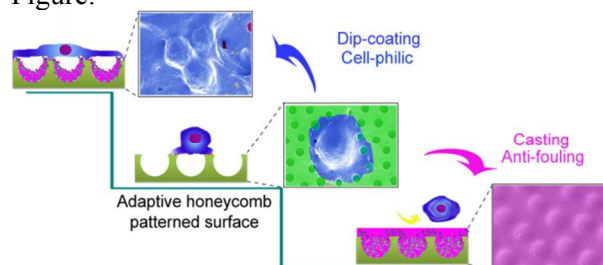
E-mail address: qhlu@sjtu.edu.cn (Q. L.); xueminlu@sjtu.edu.cn (X. L.).

1. L. E. Niklason and R. S. Langer, *Transpl. Immunol.*, 1997, **5**, 303-306.
2. K. J. L. Burg, S. Porter and J. F. Kellam, *Biomaterials*, 2000, **21**, 2347-2359.
3. J. Nikolovski and D. J. Mooney, *Biomaterials*, 2000, **21**, 2025-2032.
4. M. P. Lutolf and J. A. Hubbell, *Nat. Biotechnol.*, 2005, **23**, 47-55.
5. G. D. Prestwich, S. Bhatia, C. K. Breuer, S. L. M. Dahl, C. Mason, R. McFarland, D. J. McQuillan, J. Sackner-Bernstein, J. Schox, W. E. Tente, A. Trounson, C. K. Breuer and A. Trounson, *Sci. Transl. Med.*, 2012, **4**, 6.
6. D. G. Anderson, J. A. Burdick and R. Langer, *Science*, 2004, **305**, 1923-1924.
7. M. E. Furth, A. Atala and M. E. Van Dyke, *Biomaterials*, 2007, **28**, 5068-5073.
8. F. Xia and L. Jiang, *Adv. Mater.*, 2008, **20**, 2842-2858.
9. R. G. Flemming, C. J. Murphy, G. A. Abrams, S. L. Goodman and P. F. Nealey, *Biomaterials*, 1999, **20**, 573-588.
10. C. M. Preuss, T. Tischer, C. Rodriguez-Emmenegger, M. M. Zieger, M. Bruns, A. S. Goldmann and C. Barner-Kowollik, *J. Mater. Chem. B*, 2014, **2**, 36-40.
11. D. J. Kim, J. K. Seol, G. Lee, G. S. Kim and S. K. Lee, *Nanotechnology*, 2012, **23**, 9.
12. X. Yao, R. Peng and J. Ding, *Adv. Mater.*, 2013, **25**, 5257-5286.
13. C. S. Chen, M. Mrksich, S. Huang, G. M. Whitesides and D. E. Ingber, *Science*, 1997, **276**, 1425-1428.
14. W. Ye, Q. Shi, S. C. Wong, J. W. Hou, H. C. Shi and J. H. Yin, *Macromol. Biosci.*, 2013, **13**, 676-681.
15. Y. Ito, *Biomaterials*, 1999, **20**, 2333-2342.
16. A. S. Sarvestani, *Soft Matter*, 2013, **9**, 5927-5932.
17. H. L. Fan, P. P. Chen, R. M. Qi, J. Zhai, J. X. Wang, L. Chen, L. Chen, Q. M. Sun, Y. L. Song, D. Han and L. Jiang, *Small*, 2009, **5**, 2144-2148.
18. L. B. Koh, I. Rodriguez and S. S. Venkatraman, *Biomaterials*, 2010, **31**, 1533-1545.
19. R. S. Kane, S. Takayama, E. Ostuni, D. E. Ingber and G. M. Whitesides, *Biomaterials*, 1999, **20**, 2363-2376.
20. M. Hernandez-Guerrero and M. H. Stenzel, *Polym. Chem.*, 2012, **3**, 563-577.
21. H. M. Ma and J. C. Hao, *Chem. Soc. Rev.*, 2011, **40**, 5457-5471.
22. P. Escale, L. Rubatat, L. Billon and M. Save, *Eur. Polym. J.*, 2012, **48**, 1001-1025.
23. J. R. McMillan, M. Akiyama, M. Tanaka, S. Yamamoto, M. Goto, R. Abe, D. Sawamura, M. Shimomura and H. Shimizu, *Tissue Eng.*, 2007, **13**, 789-798.
24. T. Kawano, Y. Nakamichi, S. Fujinami, K. Nakajima, H. Yabu and M. Shimomura, *Biomacromolecules*, 2013, **14**, 1208-1213.
25. Y. Fukuhira, E. Kitazono, T. Hayashi, H. Kaneko, M. Tanaka, M. Shimomura and Y. Sumi, *Biomaterials*, 2006, **27**, 1797-1802.
26. Z. H. Nie and E. Kumacheva, *Nat. Mater.*, 2008, **7**, 277-290.
27. B. W. Muir, A. Fairbrother, T. R. Gengenbach, F. Rovere, M. A. Abdo, K. M. McLean and P. G. Hartley, *Adv. Mater.*, 2006, **18**, 3079-3081.

28. T. Kawano, M. Sato, H. Yabu and M. Shimomura, *Biomaterials Science*, 2014, **2**, 52.
29. L. Heng, R. Hu, S. Chen, M. Li, L. Jiang and B. Z. Tang, *Langmuir*, 2013, **29**, 14947-14953.
30. J. R. McMillan, M. Akiyama, M. Tanaka, S. Yamamoto, M. Goto, R. Abe, D. Sawamura, M. Shimomura and H. Shimizu, *Tissue Eng.*, 2007, **13**, 789-798.
31. A. Sanz de Leon, J. Rodriguez-Hernandez and A. L. Cortajarena, *Biomaterials*, 2013, **34**, 1453-1460.
32. D. K. S. Choy, V. D. W. Nga, J. Lim, J. Lu, N. Chou, T. T. Yeo and S.-H. Teoh, *Tissue Eng. Part A* 2013, **19**, 2382-2389.
33. M. A. Birch, M. Tanaka, G. Kirmizidis, S. Yamamoto and M. Shimomura, *Tissue Eng. Part A* 2013, **19**, 2087-2096.
34. Y. Zhang and C. Wang, *Adv. Mater.*, 2007, **19**, 913-916.
35. E. Min, K. H. Wong and M. H. Stenzel, *Adv. Mater.*, 2008, **20**, 3550-3556.
36. C. Duan, J. Gao, D. Zhang, L. Jia, Y. Liu, D. Zheng, G. Liu, X. Tian, F. Wang and Q. Zhang, *Biomacromolecules*, 2011, **12**, 4335-4343.
37. Z. Zhang, J. Ni, L. Chen, L. Yu, J. W. Xu and J. D. Ding, *Biomaterials*, 2011, **32**, 4725-4736.
38. X. J. Shi, Y. Y. Wang, D. Li, L. Yuan, F. Zhou, Y. W. Wang, B. Song, Z. Q. Wu, H. Chen and J. L. Brash, *Langmuir*, 2012, **28**, 17011-17018.
39. D. J. Menzies, A. Cameron, T. Munro, E. Wolvetang, L. Grondahl and J. J. Cooper-White, *Biomacromolecules*, 2013, **14**, 413-423.
40. Z. Zhang, M. Zhang, S. F. Chen, T. A. Horbetta, B. D. Ratner and S. Y. Jiang, *Biomaterials*, 2008, **29**, 4285-4291.
41. Z. Zhang, T. Chao, S. F. Chen and S. Y. Jiang, *Langmuir*, 2006, **22**, 10072-10077.
42. J. Ladd, Z. Zhang, S. Chen, J. C. Hower and S. Jiang, *Biomacromolecules*, 2008, **9**, 1357-1361.
43. M. J. Hancock, K. Sekeroglu and M. C. Demirel, *Adv. Funct. Mater.*, 2012, **22**, 2223-2234.
44. M. L. Carman, T. G. Estes, A. W. Feinberg, J. F. Schumacher, W. Wilkerson, L. H. Wilson, M. E. Callow, J. A. Callow and A. B. Brennan, *Biofouling*, 2006, **22**, 11-21.
45. D. W. Bechert, M. Bruse and W. Hage, *Exp. Fluids* 2000, **28**, 403-412.
46. H. Tianxian, Z. Li and D. Wenli, *Mater. Chem. Phys.*, 2011, **131**, 23-26.
47. D. Wenli, *Nature Precedings*, 2008.
48. T. Sun, L. Feng, X. Gao and L. Jiang, *Acc. Chem. Res.*, 2006, **39**, 487-487.
49. E. Cukierman, R. Pankov, D. R. Stevens and K. M. Yamada, *Science*, 2001, **294**, 1708-1712.
50. S. Schlie-Wolter, A. Ngezahayo and B. N. Chichkov, *Exp. Cell. Res.*, 2013, **319**, 1553-1561.
51. C. Fairman, J. Z. Ginges, S. B. Lowe and J. J. Gooding, *Chemphyschem*, 2013, **14**, 2183-2189.
52. S. F. Chen, L. Y. Li, C. Zhao and J. Zheng, *Polymer*, 2010, **51**, 5283-5293.
53. L. Petrone, *Adv. Colloid Interface Sci.*, 2013, **195-196**, 1-18.
54. M. Rabe, D. Verdes and S. Seeger, *Adv. Colloid Interface Sci.*, 2011, **162**, 87-106.
55. S. Chen and S. Jiang, *Adv. Mater.*, 2008, **20**, 335-338.
56. L. Heng, X. Meng, B. Wang and L. Jiang, *Langmuir*, 2013, **29**, 9491-9498.
57. E. A. Evans and D. A. Calderwood, *Science*, 2007, **316**, 1148-1153.

Table of Contents

Figure:



PS honeycomb structured surfaces were modified into both cell-philic and cell-phobic by dip-coating and casting polySBMA, respectively, which was inspired by two typically adhesive behaviours of fish skin and *Parthenocissus tricuspidata*.

Supporting Information

Biomimetic Honeycomb-patterned Surface as the Tunable Cell Adhesion Scaffold

S. S. Chen, X. M. Lu, * Y. Hu and Q. H. Lu *

Attenuate total reflectance-Fourier-transform infrared spectroscopy (ATR- FTIR) was recorded using a Perkin-Elmer Spectrum 100 (USA).

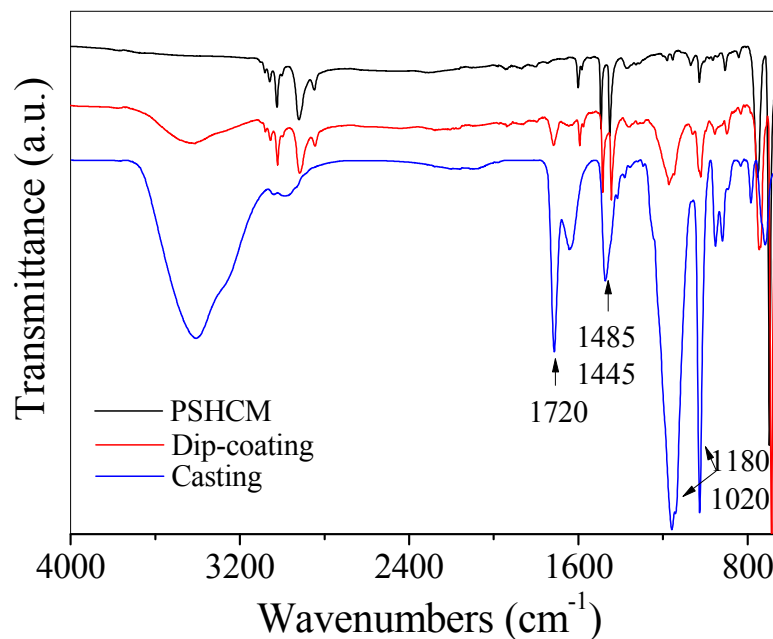


Figure S1. The ATR-FTIR spectra of PSHCM and the modified membranes by dip-coating and casting.

Similar peak information of membranes was obtained via ATR-FTIR compared with FTIR. The bands at $\nu=1180$ and 1020 cm^{-1} can be assigned to antisymmetric and symmetric vibrations of the sulfonyl group ($-\text{SO}_3$) and 1720 cm^{-1} is the typical peak of carbonyl group ($\text{C}=\text{O}$), both groups are of the SBMA segment. Moreover, an obvious difference in intensity of the two characteristic peaks, where the stretching vibration peak of $\text{C}=\text{C}$ in the benzene ring ($\nu=1490 \text{ cm}^{-1}$) is chosen as a reference, could be seen in the spectra of the two decorated membranes: the peak intensity in the spectrum of the polySBMA-decorated membrane obtained by direct casting was stronger than that in the spectrum of the dip-coated membrane, implying a difference in SBMA grafting density.

The X-ray Photoelectron Spectroscopy (XPS) was measured on PHI-5000 Versaprobe II (Japan). The scanning area is 200×200μm.

Table S1. XPS results of membranes.

Membranes	S 2p		C 1s		N 1s		O 1s	
	Peak/eV	Atomic %						
PSHCM	166.7	0.00	283.5	97.09	400.4	0.00	530.6	2.91
Dip-coating	165.75	3.36	283.5	64.82	400.4	5.80	530.6	26.02
Casting	166.7	4.22	283.5	64.79	400.4	5.51	530.6	25.68

As shown in Table S1, the peaks of polySBMA (N and S elements) can't be observed on PSHCM, which is attributing to that the chemical property of PSHCM only contains carbon and hydrogen elements. After modification by polySBMA, both on the dip-coating and casting PSHCM exhibit the information of S and N elements. The XPS furthermore demonstrated the grafting of polySBMA on the membranes.

The wettability of membranes was measured using an OCA 20 apparatus (Dataphysics, Germany).

Table S2. Water and diiodomethane contact angle

Surfaces	Water	Diiodomethane
Smooth PS	97±1°	41±1°
PS-HCM	106±5°	37±4°
Casting HCM	30±2°	56±1°
Dip-coating	25±4°	64±3°

The surface energy was calculated based on Owens, Wendt, Rabel and Kaelble (OWRK) method. The Surface free energy of water and diiodomethane was provided by Busscher as showed in Table S2.

Table S3. The surface free energy and component of water and diiodomethane

Liquids	SE(mN/m)	Dispersion(mN/m)	Polar(mN/m)
Deionized water	72.10	19.90	52.20
Diiodomethane	50.00	47.4	2.60

The OWRK method is a standard method for calculating the surface free energy of a solid from the contact angle with several liquids. In doing so, the surface free energy is divided into a polar part and a disperse part.

The OWRK equation

$$\gamma_{sl} = \delta_s + \delta_l - 2(\sqrt{\delta_s^D \cdot \delta_l^D} + \sqrt{\delta_s^P \cdot \delta_l^P})$$

And the Young's equation

$$\delta_s = \gamma_{sl} + \cos \theta \cdot \delta_l$$

Where,

γ_{sl} : Solid-liquid interfacial tension;

δ_s, δ_l : Surface energy of solid and liquid, respectively;

$\delta_s^D \cdot \delta_l^D$: Disperse part of surface energy;

$\delta_s^P \cdot \delta_l^P$: Polar part of surface energy;

$\cos \theta$: Contact angle.

The above two equations can be consolidated. When a solid was tested with two liquids whose δ_l^D and δ_l^P has been known. Three unknown parameters need to be solved, namely θ , δ_s^D and δ_s^P . The contact angles would be obtained by experiment and plugged into the equations to solve the equations.

In our systems, the surface energy results were showed in Table S3.

Table S4. Surface energy and components of membranes

Liquids	SE(mN/m)	Dispersion(mN/m)	Polar(mN/m)
Smooth PS	40.43	40.42	0.01
PS-HCM	46.07	45.31	0.76
Casting HCM	59.98	16.45	43.13
Dip-coating	69.14	11.60	57.54

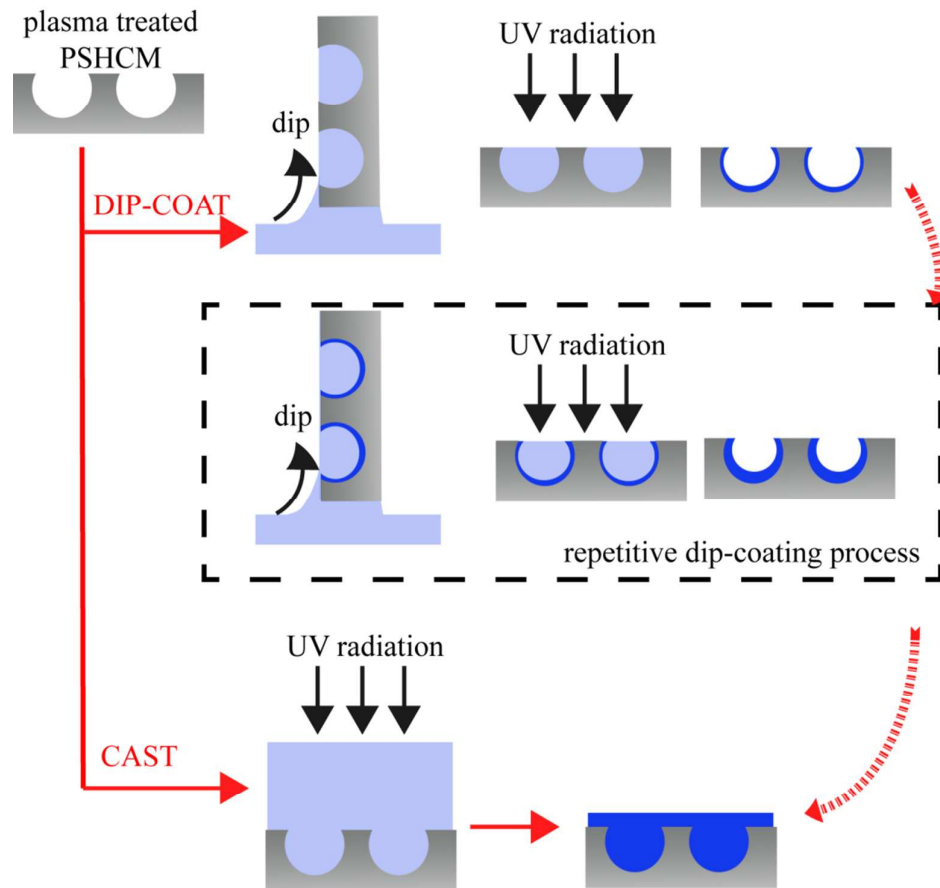


Figure S2. The Schematic illustration of the fabrication process of zwitterionic polySBMA grafted onto the honeycomb PS membrane.

The dip-coating and casting process can be applied to obtain different distribution of polySBMA as shown in Figure S1. After PSHCM being treated with plasma, the surface would be abundant with free radical. When modified by dip-coating method, the SBMA solution would aggregate in the honeycomb cavities for the capillary force. The film was further treated with UV radiation. Owing to the surficial free radical, the SBMA polymerized onto the wall of honeycomb hole. When modified by casting method, the SBMA solution would totally cover the surface of plasma treated PSHCM. After the UV radiation, the polySBMA would uniformly cover the surface. Here, a mythological repetitive dip-coating process was exhibited. If the dip-coated membrane was retreated with dip-coating process, the hole of honeycomb would be decorated with more polySBMA. The conceivable result of repetitive dip-coating membranes is that the cavities would be fully filled with polySBMA until to be uniformly covered liking casting membrane.

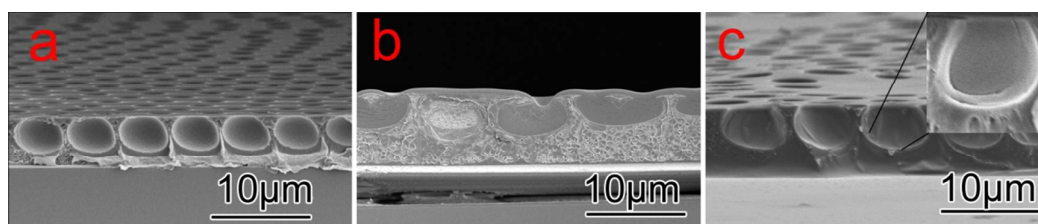


Figure S3. Cross-section SEM photographs of PSHCM (a), casting PSHCM (b) and dip-coating PSHCM (c). The hole of PSHCM after casting was filled with polySBMA, while that after dip-coating the porous structure was retained, and most of the polySBMA aggregated around the wall of the pores.

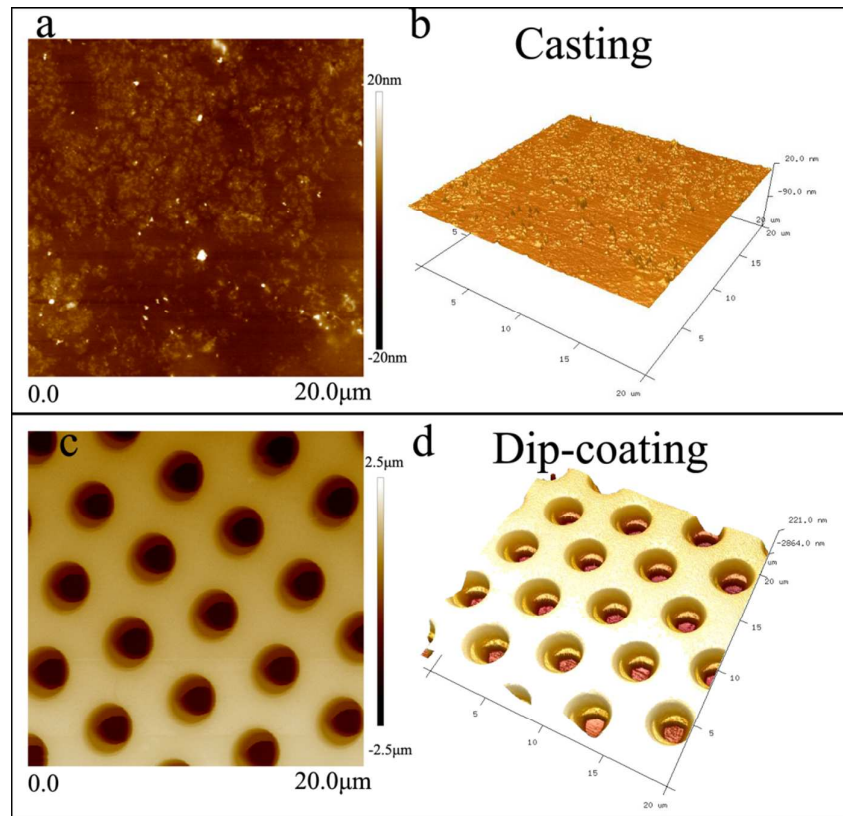


Figure S4. Plane AFM images (a,c) and 3D AFM (b,d) images of polySBMA casted PSHCM (top) and polySBMA dip-coating PSHCM (bottom). The hole of PSHCM after casting was filled with polySBMA. Thus, the AFM images showed a plane surface. While PSHCM after dip-coating retained the porous structure, and most of the polySBMA was aggregatively grafted around the hole of the pores.

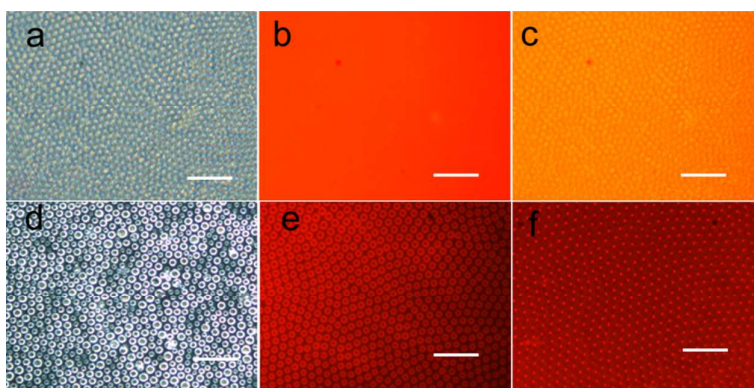


Figure S5. Fluorescence images of polySBMA modified PSHCM via casting (line 1) and dip-coating (line 2): a,d) the bright-field. b,e) fluorescent-field. c,f) bright/fluorescent composited field. Scale bar= 20 nm

PolySBMA contains a large number of ammonium ($-\text{NH}_2^+$) and sulfonic ($-\text{SO}_3^-$) groups, which could combine with the fluorescent dye (Rh-B). In contrary, the PS does not interact with Rh-B. It means that only the domain which had been decorated by polySBMA can emit fluorescent light in the exciting fluorescent field. Thus the Rh-B labelling can be applied to exemplify the distribution of polySBMA.

When observed under fluorescent field, the polySBMA casted PSHCM formed a uniform fluorescence layer. While that of dip-coated one was quite different from it. Only fluorescent circle around the honeycomb holes can be observed which indicating a micro-distribution of polySBMA. Due to the difference in refractive index between PS and polySBMA, porous structures can be observed on the casting membranes under optical field.